

# Gold and iodine diffusion in large area perovskite solar cells under illumination

*Stefania Cacovich<sup>1</sup>\*, Lucio Cinà<sup>2</sup>, Fabio Matteocci<sup>2</sup>, Giorgio Divitini<sup>1</sup>, Paul A. Midgley<sup>1</sup>, Aldo Di Carlo<sup>2</sup>, Caterina Ducati<sup>1</sup>.*

<sup>1</sup>Department of Materials Science & Metallurgy, University of Cambridge, 27 Charles Babbage road, CB3 0FS, Cambridge, UK

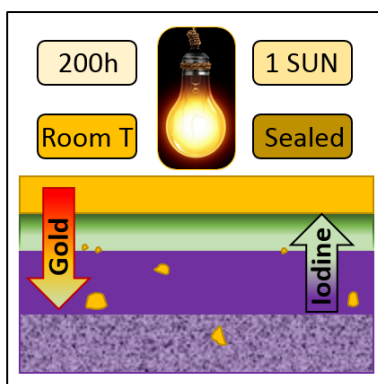
<sup>2</sup>C.H.O.S.E. (Centre for Hybrid and Organic Solar Energy), Department of Electronic Engineering, University of Rome “Tor Vergata”, via del Politecnico 1, Rome 00133,

## **Corresponding Author**

[\\*sc862@cam.ac.uk](mailto:*sc862@cam.ac.uk)

## ABSTRACT

Operational stability is the main issue hindering the commercialisation of perovskite solar cells. Here, a long term light soaking test was performed on large area hybrid halide perovskite solar cells to investigate the morphological and chemical changes associated with the degradation of photovoltaic performance occurring within the devices. Using Scanning Transmission Electron Microscopy (STEM) in conjunction with EDX analysis on device cross sections, we observe the formation of gold clusters in the perovskite active layer as well as in the TiO<sub>2</sub> mesoporous layer, and a severe degradation of the perovskite due to iodine migration into the hole transporter. All these phenomena are associated with a drastic drop of all the photovoltaic parameters. The use of advanced electron microscopy techniques and data processing provides new insights on the degradation pathways, directly correlating the nanoscale structure and chemistry to the macroscopic properties of hybrid perovskite devices.



Over the last few years, organic-inorganic perovskite based solar cells have attracted strong interest due to their excellent photovoltaic properties, resulting in an unprecedented rise in power conversion efficiency<sup>1</sup>. One of the fundamental challenges the community is facing today concerns the stability of the cells<sup>2-5</sup>. Intrinsic and extrinsic degradation processes underlying the drop in device performance have been widely investigated using macroscopic characterization tools<sup>6-8</sup>, and several studies reported humidity<sup>9, 10</sup>, temperature<sup>11, 12</sup> and light exposure<sup>13-15</sup> as responsible factors. In particular, two recently published papers highlight the presence of elemental migration within a perovskite thin film and in a state-of-the-art complete solar cell due to light exposure. De Quilletes et al. investigated the changes in the local PL (photoluminescence) intensity and PL lifetime in a methylammonium lead iodide thin film after 1 hour of light soaking<sup>16</sup>. The redistribution of the iodine content, studied via ToF-SIMS, was correlated to a local improvement in the optical properties. Elemental migration under light exposure was reported by Domansky et al. in a combined thermal and light soaking test over 15 hours, showing evidence of gold migration into the mesoporous and compact perovskite layer using a ToF-SIMS approach<sup>17</sup>.

In order to establish a direct connection between illumination and irreversible degradation of photovoltaic performance it is essential to investigate how the morphology and chemical composition of the nanostructured active layers are affected by light soaking under electrical bias. Imaging and analytical tools with high spatial resolution are necessary in order to measure changes that happen at nanometer scale.

In this work we report a study of the effect of light soaking on large area hybrid perovskite solar cells, using Scanning Transmission Electron Microscopy in conjunction with Energy Dispersive X-ray spectroscopy (STEM-EDX), and characterizing, at the nanoscale, the chemical changes that

occur within devices illuminated for 200 hours under dynamical bias. The large area solar cells (1.05 cm<sup>2</sup>) are fabricated using solvent engineering<sup>18</sup>, in an established architecture: fluorine doped tin oxide (FTO) coated glass / compact TiO<sub>2</sub> / mesoporous TiO<sub>2</sub> / perovskite / Spiro-OMeTAD/ Au. In order to improve hole transport, FK209 - a cobalt based compound - was employed as Spiro-OMeTAD dopant<sup>19</sup>. The devices were sealed according to a previously published method<sup>20</sup>, to protect the cells from contamination and moisture, thus preventing cell degradation due to extrinsic factors. In this work we investigated the behavior of an “early failed” cell, to evaluate the phenomena leading to the cell breakdown.

We compared an as-produced device aged in dark, in open circuit configuration, with an identical device that was exposed to a light soaking stability test for 200 hours, under 1 sun of illumination, at room temperature and dynamically biased at Maximum Power Point (MPP). A white light LED source was chosen in order to avoid possible degradation due to UV and IR radiation, limiting the optical excitation to the visible spectrum. The main photovoltaic parameters were recorded every 20 minutes with an I-V scan. The overall trends are reported in Figure 1a. The stability test induced a dramatic fall of the short circuit current ( $J_{sc}$ ) during the first 50 hours, together with a linear reduction of the open circuit voltage ( $V_{oc}$ ). This results in an obvious drop of the fill factor (FF) and the Power Conversion Efficiency (PCE), which decreased from the initial value of 15.89% to 0.37% after 100 hours of light exposure, showing a strong correlation with the trend of the  $J_{sc}$ . Interestingly,  $J_{sc}$  and  $R_s$  show a change in their slope at about 45 hours. At this time the cell reached a 90% of drop in efficiency and we hypothesize the activation of a new degradation phenomenon which increases the relative loss of resistance.

The effect of the light soaking stability test over the main physical processes of the device was investigated with a set of steady state and transient measurements before and after the test, as

shown in Figure 1. The J–V curves measured under 1 sun and in dark are shown in Figure 1b and c. The increase in dark current up to four decades in the low voltage range (0 to 0.5 V) where trap-assisted phenomena are generally more evident<sup>21</sup>, suggest that light soaking has induced defect states in the effective band gap of the device.

The ability of the perovskite layer to inject charges into the mesoporous TiO<sub>2</sub> layer was measured using Transient Photo-Voltage analysis (TPV)<sup>22</sup>. In particular, the open circuit voltage rise test involves monitoring the photovoltage when the device is taken from a dark steady state, to light source and monitoring the subsequent rise in photovoltage<sup>23</sup>. The concentration of the photo-injected electrons in the TiO<sub>2</sub> primarily determines the photovoltage transient profile. In this scenario, the free charge recombination processes within perovskite layer and HTM<sup>24,25</sup> reduces the build-up of electrons and, hence, the consequent dynamic response of V<sub>oc</sub>. As reported in Figure 1d, after the stress the device shows an extremely slow V<sub>oc</sub> rise profile that can be associated to degradation in the perovskite layer and its capability to inject charges into the TiO<sub>2</sub> layer. Differently, the TPV decay test (Figure 1e) was performed in order to investigate the interfacial charge-recombination dynamic and its modification after the stress test. Temporal trends were fitted with a tri-exponential decay function (dashed line). The temporal profiles show an evident decrease in the decay time that is around 3 orders of magnitude lower after the light soaking test. This results strongly confirm the activation of new recombination paths from TiO<sub>2</sub> to perovskite and HTM layers.

Complementary information regarding the recombination phenomena are extracted from the light intensity (P<sub>inc</sub>) dependence of the V<sub>oc</sub> and J<sub>sc</sub>. Figure 1f shows semi-logarithmic plots of the V<sub>oc</sub> versus light intensity for the PSC before and after the light-soaking. In particular, the fresh device shows the same slope (149 mVdec<sup>-1</sup>) over 3 decades of irradiation level. Interestingly, the

aging process introduces a suppression of the photovoltage in the low level of irradiation ( $< 10 \text{ mWcm}^{-2}$ ). As demonstrated by Gouda et al.<sup>26</sup>, at these irradiation level the increase of  $V_{oc}$  is limited by the  $\text{TiO}_2$  and the accumulation of the photo-injected electrons, similar to the dye sensitized technology. This is a clear indication of the severe photo-induced degradation of the mesoporous layer. Under intermediate and high light intensity (around 10 to  $100 \text{ mWcm}^{-2}$ ), the aged device shows a three-fold increase in the  $V_{oc}$  slope ( $475 \text{ mVdec}^{-1}$ ); further, it has been demonstrated<sup>26</sup> that in this operative region the photovoltage trend is mainly related to the Fermi level in the perovskite<sup>26</sup>. In particular, the higher  $V_{oc}$  slope suggests the activation of trap states inside the perovskite layer<sup>27</sup> that can explain the loss in the voltage decay time (Figure 1e). Similarly, the light intensity dependence of the  $J_{sc}$  is reported Figure 1g. A power law fit of the curves shows that the power index ( $\gamma$ ) is almost unity (0.97) before the stress while it reduces to 0.88 after the light-soaking. This indicates the appearance of bimolecular recombination processes induced by the light stress that degrades the charge collection capability<sup>28</sup>. Therefore, the synergetic effects of the  $\text{TiO}_2$  degradation and trap state formation inside the perovskite layer combined with the bimolecular recombination evidence lead to a premature loss in performance.

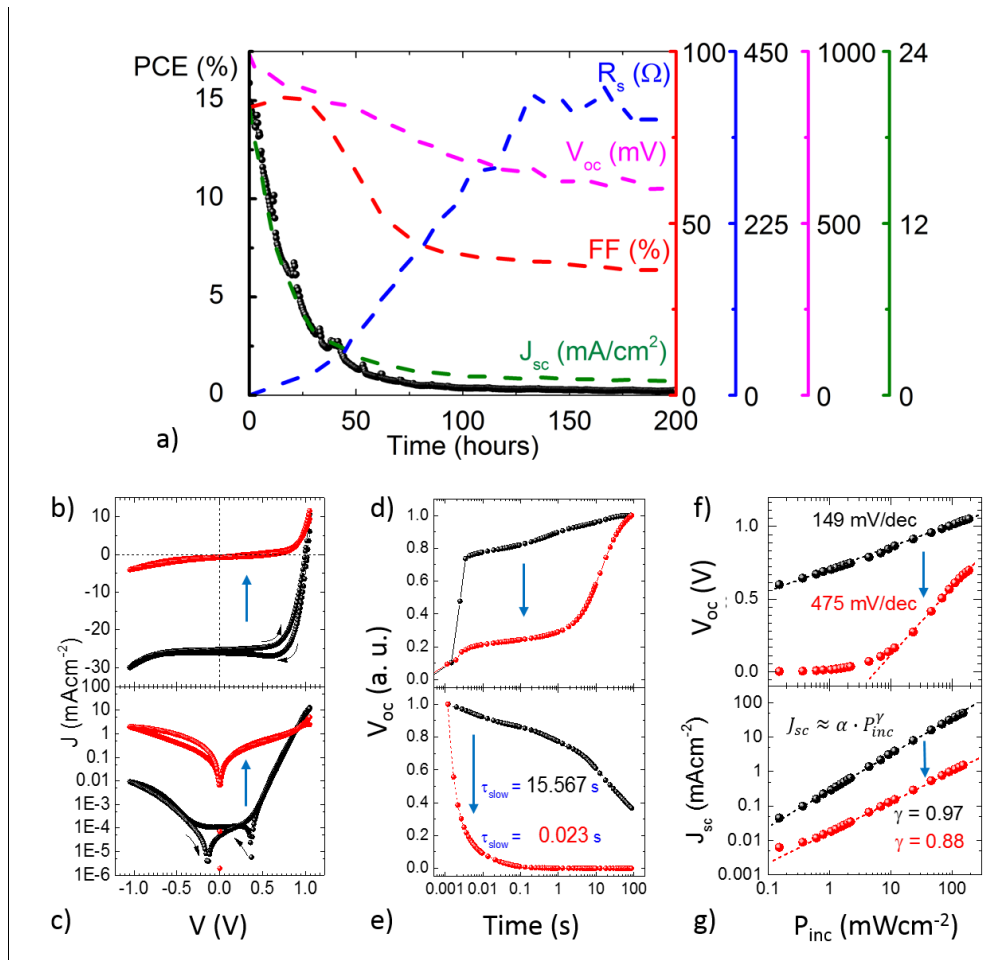


**Figure 1.** a) PCE, FF,  $J_{sc}$ ,  $V_{oc}$ ,  $R_s$  Temporal trends over the 200h stability test with MPP tracking. b-c) Illuminated and dark J-V curves measured in forward and reverse scan direction before (black) and after (red) light soaking test d) normalized TPV rise test from dark to 1 sun e) normalized TPV decay from 1 sun to dark f)  $V_{oc}$  versus the optical incident power ( $P_{inc}$ ) from 0.001 to 1.5 sun g)  $J_{sc}$  versus the  $P_{inc}$ .

The large, irreversible effects evident in the electrical characterization suggest a structural degradation of the perovskite active layer with a rise of unwanted recombination phenomena that prevent charge collection on the outer circuit. Nanoscale changes in the devices were investigated via STEM. Lamellae specimens of fresh and stressed large area cells were prepared using a focused

ion beam (FIB) approach, according to the procedure described by Langford et al.<sup>29</sup> After preparation, each cross sectional specimen was immediately transferred to a FEI Tecnai Osiris TEM/STEM operating at 200 kV. The HAADF (high angular annular dark field) STEM images of Figure 2 show a comparison of the two cells. When the thickness of the specimen is constant as in our cross sections, the intensity of HAADF STEM images is approximately proportional to the square of the atomic number<sup>30</sup>, therefore allowing a qualitative interpretation of average composition. Perovskite infiltration in the mesoporous titania scaffold layer appears incomplete and inhomogeneous in both cells, with voids of the order of 200 nm in diameter. This was not observed in small area devices<sup>18</sup> and hence it is likely due to the up-scaling of the synthesis process and characteristic to the central region of the large area devices. In Figure S1 we report cross sectional images acquired in peripheral areas of the devices, showing a more homogeneous structure. The fresh cell shows a well formed continuous perovskite layer, with an average thickness of  $145 \pm 42$  nm. We clearly observe the formation of clusters containing heavy elements in both the perovskite and the mesoporous layer after 200h of light soaking. In the stressed device the perovskite layer appears degraded, in particular at the Spiro-OMeTAD / perovskite interface, where we also notice the presence of heavy element aggregates of the diameter of tens of nanometers. The average thickness in this case decreases to a value of  $108 \pm 27$  nm and the perovskite layer appears discontinuous but smoother where still present. This severe variation in terms of average thickness might be related to the evaporation of the iodine and organic species<sup>31,32</sup>.

The chemical and physical degradation at the active layer/hole transport layer and hole transport layer/cathode interfaces has been reported as one of the first causes for the reduction of the cells performance<sup>33,34</sup>.

Additionally, to prove the validity of the sealing procedure we report HAADF STEM images of the HTL in S2. The HTL is still continuous and voids-free, indicating that no air infiltration occurred.

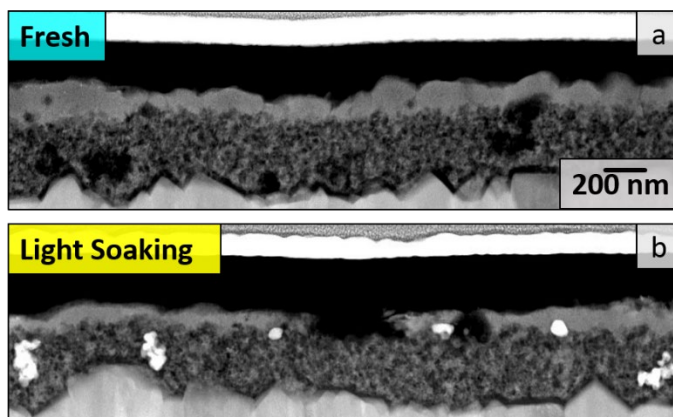


**Figure 2.** a) HAADF STEM images for a large area fresh cell and b) for a cell after 200h of light soaking.

To further investigate the nature of the gaps along the mesoporous layer as well as the chemical composition of the heavy inclusions in the stressed device we performed EDX analysis with nanometric resolution. EDX data were then treated within Hyperspy<sup>35</sup>, an open source multivariate statistical analysis tool-kit, in order to increase the signal to noise ratio and obtain more detailed and quantitative EDX maps<sup>36</sup>. The application of this method plays a key role in the analysis of data acquired with limited electron doses, representing a crucial characterization tool in the analysis of beam sensitive materials such as halide perovskites. Figure S1 shows quantitative elemental EDX maps of the representative elements in the fresh device. We note that the amount of cobalt added as Spiro-OMeTAD dopant (less than 0.1 at%), is below the detection limit of this technique. The large voids in the fresh cell appear to be filled with carbon, which might derive from different sources - the methylammonium cation in the halide perovskite, the Spiro-OMeTAD

hole transporter, or can be deposited with the electron beam during TEM analysis and sample preparation. STEM/EDX is not sensitive enough to discriminate between the carbon deriving from these possible sources.

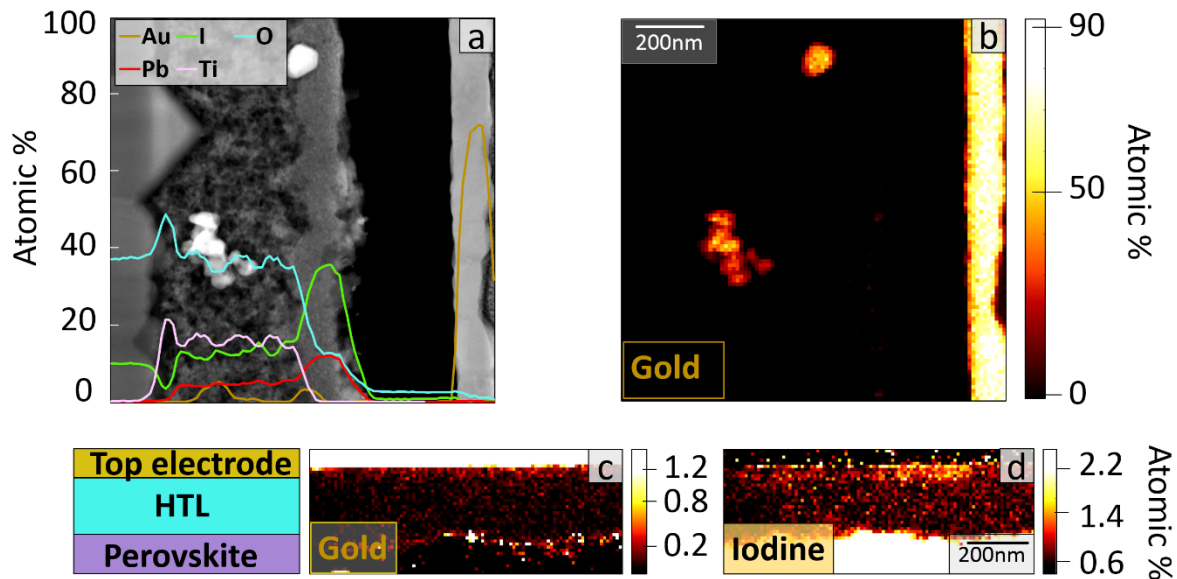


**Figure 3.** a) Quantitative EDX elemental profiles over the stressed device, superimposed on the HAADF STEM image of the area. b) Gold quantitative EDX map. c) Gold and iodine EDX maps focussing on the HTL with enhanced contrast.

Relative amounts of Au, C, I, O, Pb and Sn are determined and integrated over the width of the section of the stressed cell (i.e. along the vertical axis in Figure 3a). This phenomena was recently also observed by Domansky et al. using ToF-SIMS on cells exposed to light soaking at 70 °C for 15h<sup>17</sup>. To distinguish between the effects of the two factors - light and temperature - we performed the light soaking keeping the PSC at room temperature. Unambiguously, we find that the gold migration is induced by the light-soaking stress and in particular by electromigration. The driving

force for the gold migration lies thus in the electric field created in the device under operational conditions. The effect of the temperature on the gold migration is just to accelerate the kinetics of the process. This is confirmed by our previous investigation<sup>37</sup> where in situ measurement at different temperature stress did not show gold migration. Moreover using STEM EDX we are able not only to identify the presence of gold within both the perovskite active layer and the mesoporous layer, but also to determine the morphology of these defects within the cell. The gold EDX map in Figure 3b clearly shows that the dense clusters observed in the STEM images are gold aggregates. We speculate that these clusters agglomerate preferentially in specific regions, where defects or voids in the cell were initially present.

The use of denoising algorithms such as Non-negative Matrix Factorisation (NMF)<sup>38</sup> allowed us to investigate in detail the migration of atomic species through the Spiro-OMeTAD layer, in particular gold (Figure 3c) and iodine (Figure 3d). Under light soaking, gold appears to diffuse through the HTL and aggregate at the interface with the perovskite active layer, while iodine migrates from the perovskite layer towards the gold electrode. Iodine then accumulates at the interface HTL/gold. Therefore, we conclude that the driving force for elemental species diffusion is a combination of applied electric field and light exposure. In particular we suggest that gold migrates through the HTL and gets pinned at nucleating regions, corresponding to local defects in both the perovskite layer and the mesoporous titania scaffold, where the clusters can grow through Ostwald ripening. A similar light induced gold cluster growth mechanism has been described by Liu et al. in the context of semiconductors for nano-catalysts<sup>39</sup>. We identify gold elemental migration as one of the causes leading to the loss in performance of the cell upon light soaking. This unwanted gold diffusion might induce a degradation of the electronic properties of both the hole transport layer and the active perovskite layer. It is interesting to note that the controlled

introduction of gold nanoparticles within solar cells has been widely investigated in the context of plasmonic photovoltaic devices. Plasmonic nanoparticles have been included in the HTL<sup>40</sup>, in the perovskite layer<sup>41</sup> as well as in the mesoporous layer<sup>42</sup> obtaining an enhancement in terms of absorption and photocurrent generation of the device<sup>43</sup>. Nevertheless, the presence of gold nanoparticles has several drawbacks that need to be considered, such as the introduction of parasitic absorption, the possibility that gold aggregates act as carrier recombination centers and the risk of shorting out parts of the cell. Additionally, an uncontrolled nucleation and growth of gold nanoparticles does not allow to reach a good compromise between an increase in the spectral absorption and a potential degradation<sup>44</sup>.

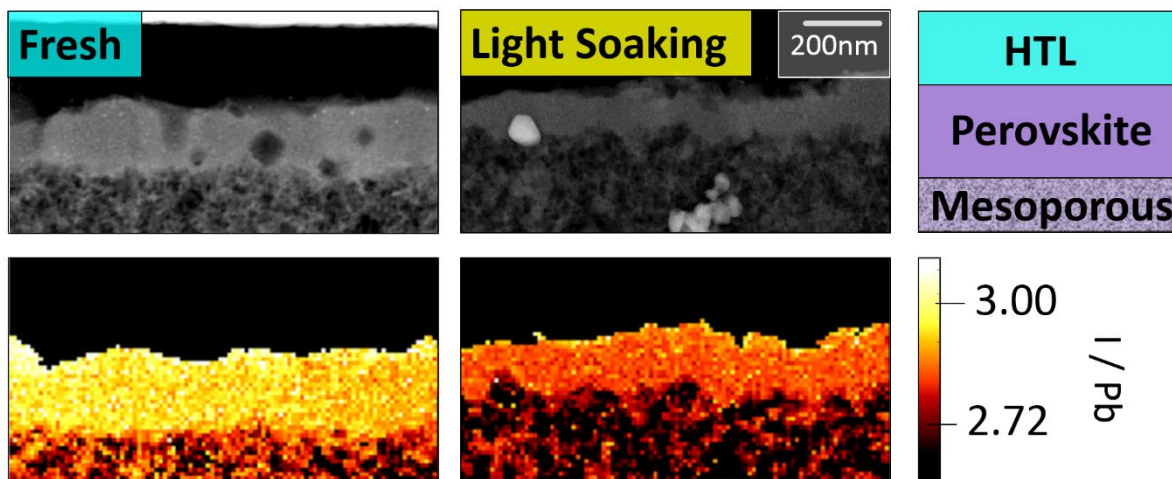


**Figure 4.** (Top) HAADF STEM images are shown next to a diagram of the cell section for fresh and stressed cells. (Bottom) Calculated atomic ratio maps for iodine/lead in the fresh and stressed cells. A mask has been applied on the HTL, setting the atomic concentrations to 0, in order to improve the clarity of the elemental ratio changes in the perovskite active layer.

Finally, we investigate the changes in the perovskite active layer composition. Figure 4 compares the relative proportions of iodine and lead in the perovskite layer for the fresh and stressed cells. In the fresh sample the ratio is close to the stoichiometric value of 3, whereas we observe a reduction down to 2.75 in the stressed cell. This is a further confirmation of the perovskite degradation due to iodine migration, causing a reduced photocurrent generation. Our results are in line with the structural modification reported by Lejitens et al.<sup>45</sup> after applying an electric field on a  $\text{CH}_3\text{NH}_3\text{PbI}_3$  thin film. The electric field created under working condition has induced the migration of iodine ions within the HTL.

The effects of a long term light soaking test under electrical bias on a large area perovskite solar cell have been investigated at the nanoscale, showing a direct link between the reduction of the photovoltaic parameters and the chemical and structural degradation of the cell. In particular we observe the formation of gold precipitates at the interface between Spiro-OMeTAD and perovskite and of bigger clusters within the perovskite active layer and the mesoporous layer. The permeation of gold inside the mesoporous  $\text{TiO}_2$  layer could result in a large increase of recombination paths for the photo-injected electrons and, hence, a decrease in the charge collection efficiency, as observed in the trends of the photovoltaics parameters in the long term test. Additionally, the obvious decrease of the short circuit current  $J_{\text{sc}}$  and the rise of the recombination processes, highlighted by both steady state and transient measurements, can be directly related to a morphological and chemical degradation of the perovskite layer due to the loss of iodine upon migration. All these phenomena lead to a decrease in photovoltaic parameters, as they affect charge generation and transport within the device.

The proven diffusion of Au and I induced by the light-soaking stress calls for a new stabilization strategies of PSC. Firstly, it is necessary to reduce this diffusion by employing alternative HTMs

(for example by using inorganic HTMs)<sup>46</sup>, replacing gold or working on interlayers<sup>17,47,48</sup>. At the same time more stable perovskite formulations should be investigated, such as the multi-cation materials that have been recently proposed<sup>49</sup>.

## ASSOCIATED CONTENT

**Supporting Information.** Experimental methods: device fabrication, sealing procedure, photovoltaic characterization, electron microscopy characterization, EDX quantitative maps, cross sectional STEM. “This material is available free of charge via the Internet at <http://pubs.acs.org>.”

## AUTHOR INFORMATION

sc862@cam.ac.uk

## Notes

The authors declare no competing financial interest.

## ACKNOWLEDGMENT

S.C., G.D., P.A.M. and C.D. thank Dr Francisco de la Peña and Dr Pierre Burdet for helpful discussions about multivariate analysis. S.C., G.D. and C.D. acknowledge funding from ERC under grant number 259619 76 PHOTO EM. G.D., P.A.M. and C.D. acknowledge financial support from the EU under grant number 77 312483 ESTEEM2. L.C., F.M., and A.D.C. acknowledge funding from EU FP7 ITN “Destiny”, the European Union’s Horizon 2020 Framework Program for Research and Innovation under Grant agreement no. 653296 (CHEOPS).

## REFERENCES

- (1) Green M.; Emery K.; Hishikawa Y.; Warta W.; Dunlop E.D. Prog. Photovolt: Res. Appl. **2016**, 24:3–11.
- (2) Zhou Y.; Zhu K. Perovskite Solar Cells Shine in the “Valley of the Sun”. *ACS Energy Lett.* **2016**, 1(1), 64–67.
- (3) Leijtens T.; Eperon G. E.; Noel N. K.; Habisreutinger S. N.; Petrozza A.; Snaith H. J. Stability of Lead Halide Perovskite. *Adv. Energy Mater.* **2015**, 5, 1500963.
- (4) Kim H.-S.; Seo J.-Y.; Park N.-G. Material and Device Stability in Perovskite Solar Cells. *ChemSusChem* **2016**, 9, 2528-2540.
- (5) Abraha Behre T.; Su W.-N.; Chen C.-H.; Pan C.-J.; Cheng J.-H.; Chen H.-M.; Tsai M.-C.; Chen, A. Aregahegn Dubaleb L.-Y.; Hwang B.-J. Organometal Halide Perovskite Solar Cells: Degradation and Stability. *Energy Environ. Sci.* **2016**, 9, 323—356.
- (6) Leguy A. M. A.; Hu Y.; Campoy-Quiles M.; Alonso M. I.; Weber L. J.; Azarhoosh P.; van Schilfgaarde M.; Weller M. T.; Bein T.; Nelson J.; Docampo P.; Barnes P. R. F. Reversible Hydration of  $\text{CH}_3\text{NH}_3\text{PbI}_3$  in Films, Single Crystals, and Solar Cells. *Chem. Mater.* **2015**, 27, 3397–3407.
- (7) Yang J.; Siempelkamp B.D.; Kelly T.L. Investigation of  $\text{CH}_3\text{NH}_3\text{PbI}_3$  Degradation Rates and Mechanisms in Controlled Humidity Environments Using *in Situ* Techniques *ACS Nano*, 2015, 9 (2), 1955-1963.

(8) Schlipf J.; Docampo P.; Schaffer C.J.; Körstgens V.; Bießmann L.; Hanusch F.; Giesbrecht N.; Bernstorff S.; Bein T.; Müller-Buschbaum P. A Closer Look into Two-Step Perovskite Conversion with X-ray Scattering. *J. Phys. Chem. Lett.* **2015**, *6*, 1265-1269.

(9) Habisreutinger S. N.; Leijtens T.; Eperon G. E.; Stranks S. D.; Nicholas R. J.; Snaith H. J. Carbon Nanotube/Polymer Composites as a Highly Stable Hole Collection Layer in Perovskite Solar Cells. | *Nano Lett.* **2014**, *14*, 5561–5568.

(10) Han Y.; Meyer S.; Dkhissi Y.; Weber K.; Pringle J. M.; Bach U.; Spiccia L.; Cheng Y.-B. Degradation observation of encapsulated planar CH<sub>3</sub>NH<sub>3</sub>PbI<sub>3</sub> perovskite solar cells at high temperatures and humidity. *J. Mater. Chem. A* **2015**, *3*, 8139.

(11) B. Conings, J. Drijkoningen, N. Gauquelin, A. Babayigit, J. D’Haen, L. D’Olieslaeger, A. Ethirajan, J. Verbeeck, M. Manca, E. Mosconi, et al. Intrinsic Thermal Instability of Methylammonium Lead Trihalide Perovskite. *Adv. Energy Mater.* **2015**, *5*, 1500477.

(12) Misra R. K.; Aharon S.; Li B.; Mogilyansky D.; Visoly-Fisher I.; Etgar L.; Katz E. A. Temperature – and Component- Dependent Degradation of Perovskite Photovoltaic Materials under Concentrated Sunlight. *J. Phys. Chem. Lett.* **2015**, *6*, 326–330.

(13) Bryant D.; Aristoudou N.; Pont S.; Sanchez-Molina I.; Chotchunangatchaval T.; Wheeler S.; R. Durrant J. R.; Haque S. A. Light and Oxygen Induced Degradation Limits the Operational Stability of Methylammonium Lead Triiodide Perovskite Solar Cells. *Energy Environ. Sci.* **2016**, *9*, 1655-1660.

(14) Wei D.; Wang T.; Ji J.; Li M.; Cui P.; Li Y.; Li G.; Mbengue J.M.; Song D. Photo-Induced Degradation of Lead Halide Perovskite Solar Cells caused by the Hole Transport Layer/Metal Electrode Interface. *Journal of Materials Chemistry A* **2016**, *4*, 1991-1998.

(15) Law C.; Miseikis L.; Dimitrov S.; Shakya-Tuladhar P.; Li X.; Barnes P.R.F.; Durrant J.; O'Regan B.C.; Performance and Stability of Lead Perovskite/TiO<sub>2</sub>, Polymer/PCBM, and Dye Sensitised Solar Cells at Light Intensities up to 70 Suns. *Advanced Materials* **2014**, *26*, 6268-6273.

(16) deQuilletes D. W.; Zhang W.; Burlakov V.M.; Graham D.J.; Leijtens T.; Osherov A.; Bulovic V.; Snaith H.J.; Stranks S.D. Photo-Induced Halide Redistribution in Organic-Inorganic Perovskite Films. *Nat. Commun.* **2016**, *7*, 11683.

(17) Domanski K.; Correa-Baena J.-P.; Mine N.; Nazeeruddin M. K.; Abate A.; Saliba M.; Tress W.; Hagfeld A.; Grätzel M. Not All That Glitters is Gold: Metal Migration-Induced Degradation in Perovskite Solar Cells. *ACS Nano* **2016**, *10* (6), 306-6314.

(18) Jeon N.J.; Noh J.H.; Kim Y.C.; Yang W.S.; Ryu S.; Seok S.I. Solvent engineering for high-performance inorganic-organic hybrid perovskite solar cells. *Nat. Mater.* **2014**, *13*, 897-903.

(19) Ganesan P.; Fu K.; Gao P.; Raabe I.; Schenk K.; Scopelliti R.; Luo J.; Wong L. H.; Grätzel M.; Nazeeruddin M. K. A Simple Spiro-Type Hole Transporting Material for Efficient Perovskite Solar Cells. *Energy Environ. Sci.* **2015**, *8*, 1986-1991.

(20) Matteocci F.; Cinà L.; Lamanna E.; Cacovich S.; Divitini G.; Midgley P.A.; Ducati C.; Di Carlo A. Encapsulation for Long-Term Stability Enhancement of Perovskite Solar Cells *Nano Energy* **2016**, *30*, 162-172.

(21) Wetzelaer G.-J. A. H.; Scheepers M.; Sempere A. M.; Momblona C.; Avila J; Bolink H. J. Trap-Assisted Non-Radiative Recombination in Organic-Inorganic Perovskite Solar Cells. *Adv. Mater.* **2015**, *27*, 1837–1841.

(22) O'Regan B. C.; Bakker K.; Kroeze J.; Smit H.; Sommeling P.; Durrant J. R. Measuring Charge Transport from Transient Photovoltage Rise Times. A New Tool to Investigate Electron Transport in Nanoparticle Films. *J. Phys. Chem. B* **2006**, *110* (34), 17155-17160.

(23) Barnes P. R. F.; Miettunen K.; Li X.; Anderson A. Y.; Bessho T.; Grätzel M.; O'Regan B. C. Interpretation of Optoelectronic Transient and Charge Extraction Measurements in Dye-Sensitized Solar Cells. *Adv Mater.* **2013**, *25*, 1881.

(24) Marin-Beloqui J. M. ; Lanzetta L.; Palomares E. Decreasing Charge Losses in Perovskite Solar Cells Through mp-TiO<sub>2</sub> / MAPI Interface Engineering. *Chem. Mater.* **2016**, *28* (1), 207–213.

(25) Bi D; Boschloo G.; Hagfeldt A.; Johansson E. M. J. Effect of Different Hole Transport Materials on Recombination in CH<sub>3</sub>NH<sub>3</sub>PbI<sub>3</sub> Perovskite-Sensitized Mesoscopic Solar Cells. *J. Phys. Chem. Lett.* **2013**, *4* (9), 1532–1536.

(26) Gouda L.; Gottesman R.; Ginsburg A.; Keller D. A.; Haltzi E.; Hu J.; Tirosh S.; Anderson A. Y.; Zaban A.; Boix P. P. Open Circuit Potential Build-Up in Perovskite Solar Cells from Dark Conditions to 1 Sun. *J. Phys. Chem. Lett.* **2015**, *6* (22), 4640–4645.

(27) You J.; Hong Z.; Yang. Y. M.; Chen Q.; Cai M.; Song T.-Z.; Chen C.-C.; Lu S.; Liu Y.; Zhou H.; Yang Y. Low Temperature Solution-Processed Perovskite Solar Cells with High Efficiency and Flexibility. *ACS Nano*, **2014**, *8* (2), 1674–1680.

- (28) Shao S.; Chen Z.; Fang H.-H., ten Brink G. H., D. Bartesaghi; Adjokatse S.; Koster L. J. A.; Kooi B. J.; Facchetti A.; Loi M. A. N-type Polymers as Electron Extraction Layers in Hybrid Perovskite Solar Cells with Improved Ambient Stability. *J. Mater. Chem. A*, **2016**, *4*, 2419.
- (29) Langford R. M.; Rogers M. In situ Lift-Out: Steps to improve yield and a comparison with other FIB TEM sample preparation techniques. *Micron* **2008**, *39*, 1325–1330.
- (30) Nellist P.D.; Pennycook S.J. The Principles and Interpretation of Annular Dark-Field Z-Contrast Imaging. *Adv. Imaging Electron Phys.* **2000**, *113*, 147–203.
- (31) Deretzis I.; A. Alberti A.; Pellegrino G.; Smecca E.; Giannazzo F.; Sakai N.; Miyasaka T.; A. La Magna A. *Appl. Phys. Lett.* **2015**, *106*, 131904.
- (32) Han Y.; Meyer S.; Dkhissi Y.; Weber K.; Pringle J. M.; Bach U.; Spiccia L.; Cheng Y.-B. *J. Mater. Chem. A*, **2015**, *3*(15), 8139–8147.
- (33) Guerrero A.; You J.; Aranda C.; Soo Kang Y.; Garcia-Belmonte G.; Zhou H.; Bisquert J.; Yang Y. Interfacial Degradation of Planar Lead Halide Perovskite Solar Cells. *ACS Nano* **2016**, *10*, 218–224.
- (34) Carrillo J.; Guerrero A.; Rahimnejad S.; Almora O.; Zarazua I.; Mas-Marza E.; Bisquert J.; Garcia Belmonte G. Ionic Reactivity at Contacts and Aging of Methylammonium Lead Triiodide Perovskite Solar Cells. *Adv. Energy Mater.* **2016**, *6*, 1502246
- (35) de la Peña F.; Burdet P.; Sarahan M.; Ostasevicius T.; Taillon J.; Eljarrat A.; Mazzucco S.; Fauske V.T.; Donval G.; Zagonel L.F. et al. Hyperspy 0.8: Hyperspectral data analysis toolbox, doi: 10.5281/zenodo.16850, **2015**.

(36) Cacovich S.; Divitini G.; Ireland C.; Matteocci F.; Di Carlo A.; Ducati C. Elemental Mapping of Perovskite Solar Cells by Using Multivariate Analysis: An Insight into Degradation Processes. *ChemSusChem* **2016**, *8*, 2673-2678.

(37) Divitini G.; Cacovich S.; Matteocci F.; Cinà L.; Di Carlo A.; Ducati C. *In situ* Observation of Heat-Induced Degradation of Perovskite Solar Cells. *Nature Energy* **2016**, *1*, 15012.

(38) Pauca V.P.; Pipera J.; Plemmons R.J. Nonnegative Matrix Factorization for spectral data analysis. *Linear Algebra and its Applications* **2006**, *416*, 29-47.

(39) Liu S.; Xu Y.-J. Photo-Induced transformation process at gold clusters-semiconductor interface: Implications for the complexity of gold clusters-based photocatalysis. *Sci. Rep.* **6**, 22742.

(40) Seul Lee D.; Kim W.; Geun Cha B.; Kwon J.; June Kim S.; Kim M.; Kim J.; Hwan Wang D.; Hyeok Park J. Self-Position of Au NPs in Perovskite Solar Cells: Optical and Electrical Contribution. *ACS Appl. Mater. Interfaces* **2016**, *8* (1), pp 449–454.

(41) Xu D.; Liu D.; Xie T.; Cao Y.; Wang J.-G.; Ning Z.-J.; Long Y.-T.; Tiana H. Plasmon Resonance Scattering at Perovskite  $\text{CH}_3\text{NH}_3\text{PbI}_3$ . *Chem. Commun.* **2016**, *52*, 9933—9936.

(42) Yuan Z.; Wu Z.; Bai S.; Xia Z.; Xu W.; Song T.; H. Wu; Xu L.; Si J.; Jin Y.; Sun B. Perovskite Solar Cells: Hot-Electron Injection in a Sandwich  $\text{TiO}_x$ -Au- $\text{TiO}_x$  Structure for High-Performance Planar Perovskite Solar Cells. *Adv. Energy Mater.* **2015**, *5*, 1500038.

- (43) Carretero-Palacios S.; Jimenez-Solano A.; Miguez H. Plasmonic Nanoparticles as Light-Harvesting Enhancers in Perovskite Solar Cells: A User's Guide. *ACS Energy Lett.* **2016**, *1*, 323-331.
- (44) Arinze E. S.; Qiu B.; Nyirjesy G.; Thon S. M. Plasmonic Nanoparticle Enhancement of Solution-Processed Solar Cells: Practical Limits and Opportunities. *ACS Photonics* **2016**, *3*, 158–173.
- (45) Leijtens T.; Eric T. Hoke E. T.; Grancini G.; Slotcavage D. J.; Eperon G. E.; Ball J. M.; De Bastiani M.; Bowring A. R.; Martino N.; Wojciechowski K.; McGehee M. D.; Henry J. Snaith H.J.; Petrozza A. Mapping Electric Field-Induced Switchable Poling and Structural Degradation in Hybrid Lead Halide Perovskite Thin Films. *Adv. Energy Mater.* **2015**, *5*, 1500962.
- (46) Wu Q.; Xue C.; Li Y.; Zhou P.; Liu W.; Zhu J.; Dai S.; Zhu C.; Yang S. Kesterite Cu<sub>2</sub>ZnSnS<sub>4</sub> as a Low-Cost Inorganic Hole-Transporting Material for High-Efficiency Perovskite Solar Cells. *ACS Appl. Mater. Interfaces* **2015**, *7* (51), 28466–28473.
- (47) Agresti A.; Pescetelli S.; Taheri B.; Del Rio Castillo A. E.; Cinà L.; Bonaccorso F.; Di Carlo A. Graphene-Perovskite Solar Cells Exceed 18% Efficiency: A Stability Study. *ChemSusChem* **2016**, *8*, 2609-2619.
- (48) Sanehira E. M.; Tremolet de Villers B. J.; Schulz P.; Reese M. O.; Ferrere S.; Zhu K.; Lin L. Y.; Berry J. J.; Luther J. M. Influence of Electrode Interfaces on the Stability of Perovskite Solar Cells: Reduced Degradation Using MoO<sub>x</sub>/Al for Hole Collection. *ACS Energy Lett.* **2016**, *1*, 38–45.

(49) Saliba M.; Matsui T.; Domanski K.; Seo J-Y; Ummadisingu A.; Zakeeruddin S. M.; Correa-Baena J-P; Tress W.R.; Abate A.; Hagfeldt A; Grätzel M. Incorporation of Rubidium Cations into Perovskite Solar Cells Improves Photovoltaic performance. *Science* **2016**, *354*, 6309, 206-209.